

# **DAMAGE AND FRACTURE IN CREEP OF MAGNESIUM ALLOY-BASED COMPOSITES**

V. Sklenicka, M. Pahutova, M. Svoboda, K. Kucharova and I. Podstranska

Institute of Physics of Materials, Academy of Sciences of the Czech Republic  
Zizkova 22, CZ-616 62 Brno, Czech Republic

## **ABSTRACT**

A comparison between the creep characteristics of AZ 91 and QE 22 alloys reinforced with 20 vol.%Al<sub>2</sub>O<sub>3</sub> short fibres and unreinforced matrix alloys shows that creep strengthening in the composites arises mainly from the existence of an effective load transfer. High values of load transfer estimated for the composites indicating good fibre/matrix interface bonding together with no substantial breakage of fibres during creep exposure lead to the conclusion that the use of alumina short fibres is very effective in improving the creep properties of Mg-based composites. However, the abrupt fracture occurring shortly after the end of the lengthy primary stage of creep at very high stresses implies the existence of a critical weakening and/or damage of the matrix/fibre interface corresponding to the ultimate state of load transfer.

## **KEYWORDS**

Mg-based composite, short-fibre composite, creep, creep damage, creep fracture, fibre breakage, load transfer, interface debonding.

## **INTRODUCTION**

There has been a dramatically increased usage of magnesium alloys in the past ten years by the automotive industry. This usage is projected to continue a large growth as automakers continue to strive for better fuel economy with reduced emission [1]. To achieve further substantial increase in usage in automotive industry, magnesium alloys must be utilized in engine and transmission components. These applications require better high temperature strength and creep resistance than it is possible with currently available commercial magnesium alloys.

A considerable improvement in the creep properties of magnesium alloys can be potentially achieved by short-fibre ceramic reinforcements (discontinuous metal matrix composites - MMCs) [2-4]. The creep properties of Mg-based composites [3-5] have received only limited attention. However, these studies are sufficient to allow some preliminary predictions on the deformation mechanisms which are significant in the creep process in Mg-based composites. By contrast, very little information is available on the creep damage mechanisms and creep fracture processes in discontinuous magnesium matrix composites.

This work reports the experimental results obtained in an investigation of the high temperature creep fracture behaviour of AZ 91 and QE 22 magnesium alloys reinforced with 20 vol.%Al<sub>2</sub>O<sub>3</sub> (Saffil) short fibres. The objective of the present research is a further attempt to clarify the creep damage and fracture mechanisms in short-fibre reinforced magnesium-based composites.

# EXPERIMENTAL DETAILS

All experimental materials used in the study were fabricated at the Department of Materials Engineering and Technology, Technical University of Clausthal, Germany. Short fibre reinforced and unreinforced blocks of the most common alloy AZ 91 (Mg-9wt%Al-1wt%Zn-0.3wt%Mn) and the high strength silver-containing alloy QE 22 (Mg-2.5wt%Ag-2.0wt%Nd rich rare earths-0.6wt%Zr) were produced by squeeze casting. The fibre preform consisted of planar randomly distributed  $\delta$ -alumina short fibres (Saffil fibres from ICL, 97%  $\text{Al}_2\text{O}_3$ , 3% $\text{SiO}_2$ ,  $\sim 3 \mu\text{m}$  in diameter with varying lengths up to an estimated maximum of  $\sim 150 \mu\text{m}$ ). The final fibre fraction after squeeze casting in both composites was about 20 vol.%. For convenience, the composites are henceforth designated AZ 91 - 20 vol.% $\text{Al}_2\text{O}_3(\text{f})$  and QE 22 - 20 vol.% $\text{Al}_2\text{O}_3(\text{f})$  where f denotes fibre. An unreinforced AZ 91 matrix alloy and its composite were subjected to a T6 heat treatment (anneal for 24 h at 688 K, air cool and then age for 24 h at 443 K). The QE 22 monolithic alloy and its composite were given the following T6 heat treatment: anneal for 6 h at 803 K, air cooling and ageing for 8 h at 477 K. Flat tensile creep specimens were machined from the blocks so that the longitudinal specimen axes were parallel to the plane in which the long axes of the fibres were preferentially situated for the squeeze-cast composites. Constant stress tensile creep tests were carried out at temperatures from 423 to 523 K and at the applied stresses ranged from 10 to 200 MPa [3,5]. Creep tests were performed in purified argon. The creep elongations were measured using a linear variable differential transducer and they were continuously recorded digitally and computer processed. Following creep testing, samples were prepared for examination by transmission electron microscopy (TEM). Observations were performed using a Philips CM 12 TEM/STEM transmission electron microscope with an operating voltage of 120 kV, equipped with EDAX Phoenix X-ray microanalyser. Fractographic details were investigated using light microscopy and scanning electron microscopy (Philips SEM 505 microscope).

## EXPERIMENTAL RESULTS

### Creep results

Figure 1 shows selected creep curves in the form of strain,  $\epsilon$ , versus time,  $t$ , for the AZ 91 alloy and its composite for the creep tests conducted at an absolute temperature  $T$  of 423 K under comparable levels of the applied stress  $\sigma$ . As demonstrated by the figure, significant differences were found in the creep behaviour of the composite when compared to its matrix alloy. First, the presence of the reinforcement leads to a substantial decrease in the creep plasticity, which is proved by the values of the total strains to fracture for the composite. Second, the composite exhibits markedly longer creep life than the alloy at the entire stress range used. Third, the shapes of creep curves for the composite and the alloy differ considerably. It should be mentioned that the creep curves shown in Fig. 1 do not clearly indicate the individual stages of creep. However, these standard  $\epsilon$  vs.  $t$  curves can be easily replotted in the form of the strain rate,  $\dot{\epsilon}$ , versus time,  $t$ , as shown in Fig. 2, Fig. 2a presents the  $\log \dot{\epsilon} - t$  curves for a temperature of 423 K and a stress of 100 MPa for both materials. It is apparent that neither curve exhibits a well-defined steady stage. In fact, this stage is reduced to an inflection point of the  $\dot{\epsilon}$  versus  $t$  curve. Despite this similarity, the occurrence of a primary stage followed by a tertiary stage of creep in the matrix alloy is in a striking contrast with the nature of the creep curve in the composite. The latter curve shows the primary stage is fairly extensive and represents practically the whole creep test. A minimum in the creep rate is reached just before final fracture and the presence of a tertiary stage is not well-defined. This difference in the shapes of the  $\dot{\epsilon} - t$  creep curves in the matrix alloy and in the composite is confirmed and perhaps more clearly illustrated in Fig. 2b for the tests conducted at the same temperature of 473 K and stress of 80 MPa. Inspection suggests that creep in the composite is again dominated by fairly extensive primary stage. On the other hand, an extremely short primary creep in the matrix alloy is followed by a lengthy tertiary stage. The creep data of the AZ 91 alloy and the AZ 91 - 20 vol.%  $\text{Al}_2\text{O}_3(\text{f})$  composite and the QE 22 alloy and the QE 22 - 20 vol.% $\text{Al}_2\text{O}_3$  composite at 423, 473 and 523 K are shown in Fig. 3 where the minimum creep rate,  $\dot{\epsilon}_m$ , is plotted against the applied stress,  $\sigma$ , on a logarithmic scale. Inspection of the creep data in Fig. 3 leads to two observations. First, the composites exhibit better creep resistance than the monolithic alloys over the entire stress range used; the minimum creep rate for the composite is about two to three orders of magnitude less than that of the

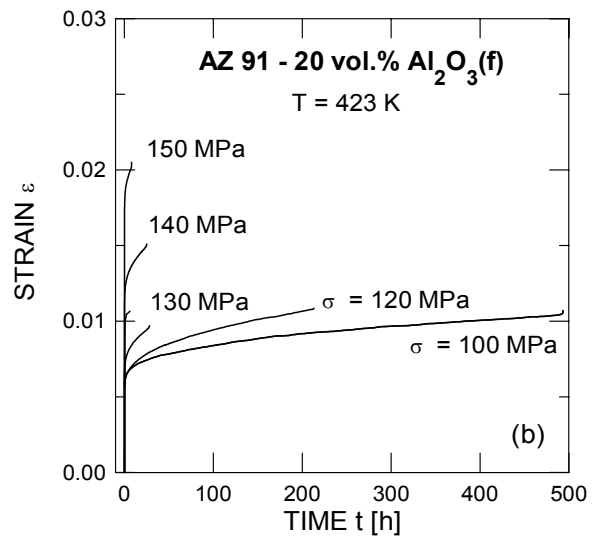
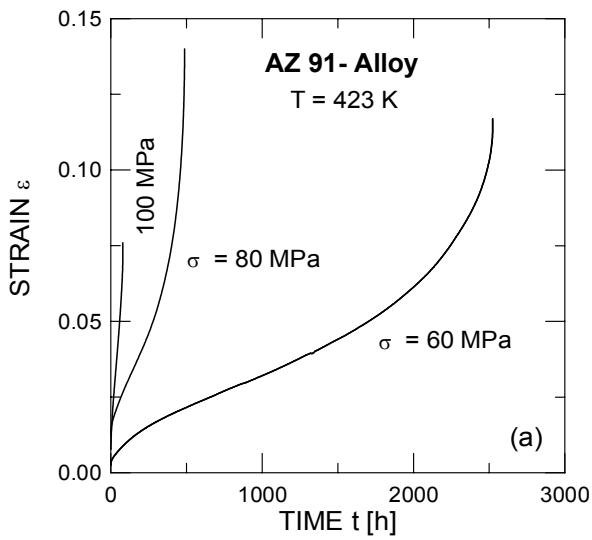


**Figure 1a,b:** Creep curves at 423 K for (a) the AZ 91 alloy, and (b) the AZ 91-20 vol.%Al<sub>2</sub>O<sub>3</sub>(f) composite.

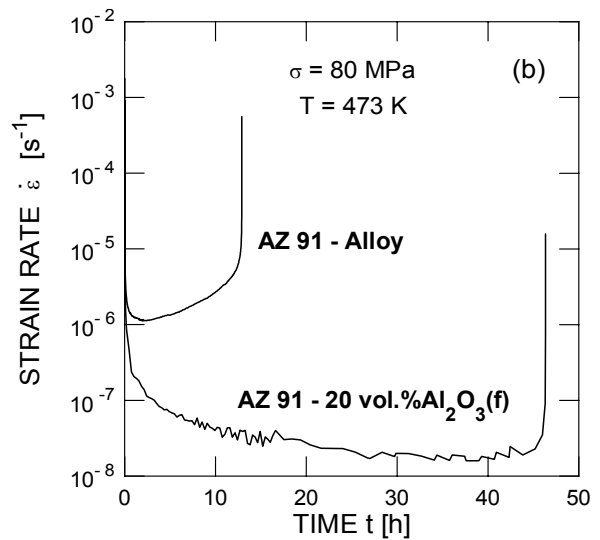
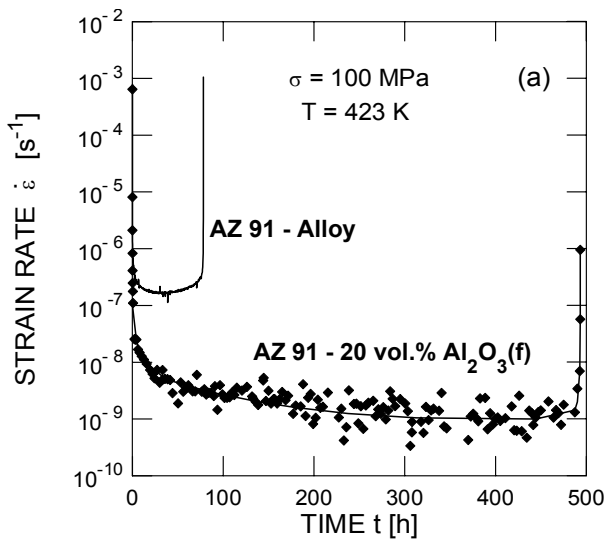


**Figure 2a,b:** Strain rate versus time for the AZ 91 alloy and the AZ 91-20vol.%Al<sub>2</sub>O<sub>3</sub>(f) composite (a) at 423 K and 100 MPa, and (b) at 473 K and 80 MPa.

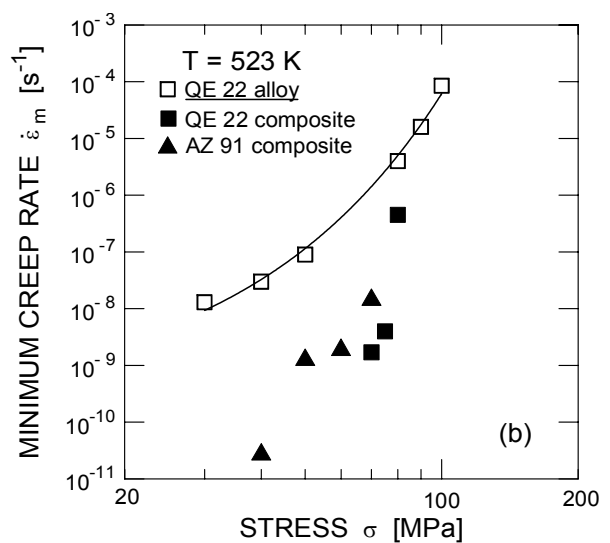
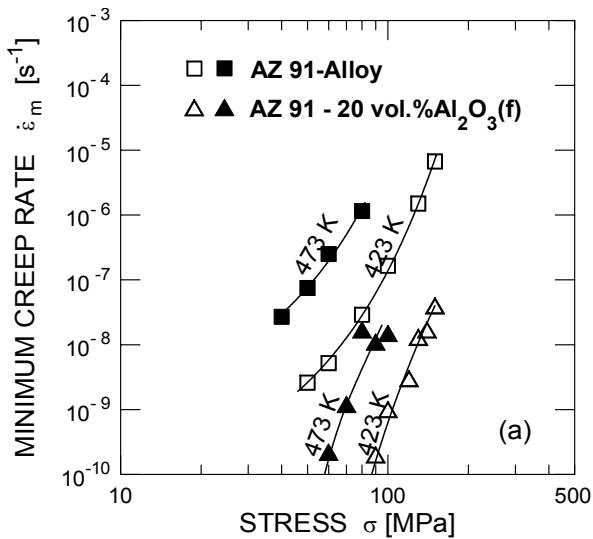


**Figure 3a,b:** Stress dependences of minimum creep rate for (a) AZ 91 alloy and its composite at 423 and 473 K, and (b) QE 22 alloy and both composites at 523 K.

unreinforced alloy. Second, as depicted in Fig. 3a, the stress dependences of the minimum creep rates for both materials are different in trend, which is clearly demonstrated by the characteristic curvatures on the inherent curves at low stress. While the slopes and therefore the apparent stress exponents,  $n_a = (\partial \ln \dot{\epsilon} / \partial \ln \sigma)_T$ , for the alloy slightly decrease with decreasing applied stress, the curvatures for the composite increase with decreasing applied stress. Such an increase of the apparent stress exponent at low stresses is usually considered to be indicative of the presence of a threshold stress representing a lower limiting stress below which creep cannot occur [3,4]. Third, the creep resistance of the QE 22 - 20 vol.%  $\text{Al}_2\text{O}_3(\text{f})$  composite seems to be essentially equal to the creep resistance of the AZ 91 - 20 vol.%  $\text{Al}_2\text{O}_3(\text{f})$  composite (Fig. 3b). The double logarithmic plots of the time to fracture  $t_f$  as a function of the applied stress  $\sigma$  at a temperature of 423 and 473 K are shown in Fig. 4a for the AZ 91 alloy and its composite. It is clear from these plots that the creep life of the AZ 91 - 20 vol.%  $\text{Al}_2\text{O}_3(\text{f})$  composite is an order of magnitude longer than that of the unreinforced AZ 91 alloy. However, this difference consistently decreases with increasing applied stress and there is a tendency for the reinforcement to have no significant effect on the lifetime at the higher stresses. In fact, inspection of Fig. 4a reveals that at stresses higher than 200 MPa the creep life of the composite is essentially equal to that of the monolithic AZ 91 alloy. The same conclusion can be drawn from Fig. 4b. Independent of the testing temperature, both composites (AZ 91 - 20 vol.%  $\text{Al}_2\text{O}_3(\text{f})$  and QE 22 - 20 vol.%  $\text{Al}_2\text{O}_3(\text{f})$ ) exhibit superior creep resistance compared to their unreinforced alloys. It should be noted that no substantial difference in lifetime was found between both composites under the same creep loading conditions. The presence of the reinforcement leads to a substantial decrease in the creep plasticity. The values of the strain to fracture in both composites are only 1 - 2%, independent of stress and temperature. By contrast, the values of the strain to fracture in the monolithic alloys are markedly higher, typically 10 - 15% in the AZ 91 alloy and up to 30% in the QE 22 alloy.

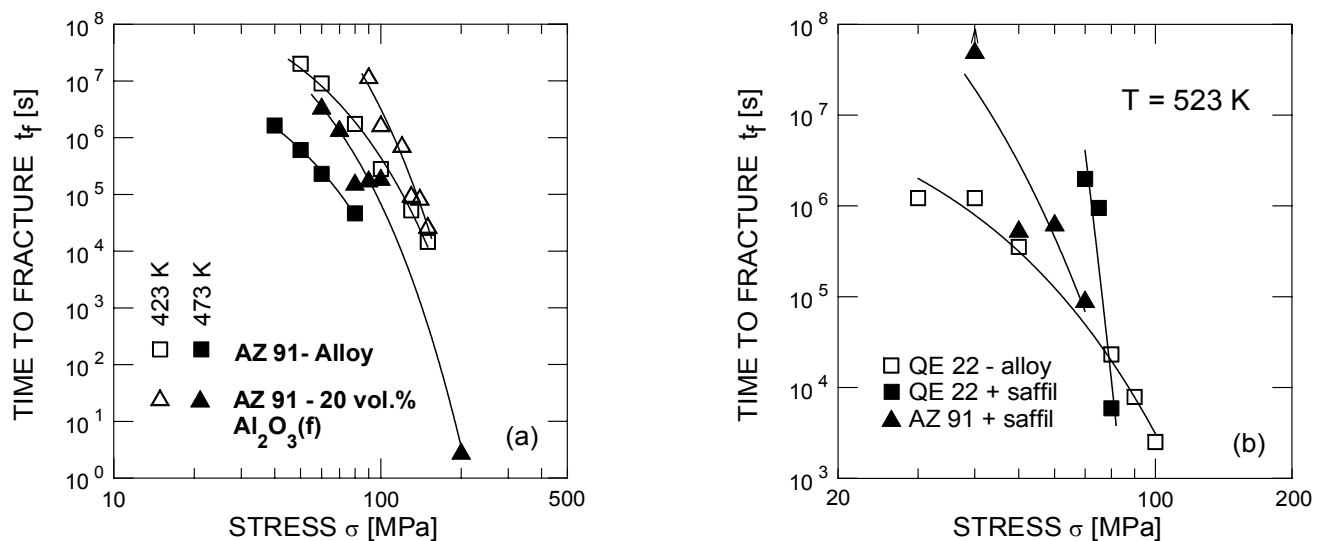


**Figure 4a,b:** Stress dependences of times to fracture for (a) AZ 91 alloy and its composite at 423 K and 473 K and (b) QE 22 alloy and both composites at 523 K.

## Fractography

Creep behaviour and the creep plasticity of material can be substantially influenced by the development of creep damage and fracture processes. The longitudinal metallographic sections cut from the gauge length of creep fractured specimens were examined using optical microscopy and SEM to evaluate creep damage. No intergranular creep cavitation has been revealed in the monolithic alloys; all the specimens failed in intergranular and/or interdendritic manner without necking. Fractographic investigations of the composites did not reveal either substantial creep fibre cracking and breakage or any debonding at the interface between the fibres and the matrix due to creep (Figure 5). It should be emphasized that these effects were restricted to a region very near the fracture path (Figure 6) suggesting that fibre breakage occurs by the propagation of the main creep crack during the final stage of the creep fracture process. Even careful investigation of the fibre-matrix interface by TEM revealed no extensive debonding (Figure 5c). Rather, the enhanced precipitation of the  $\beta$  phase on the alumina fibres and some interconnection of fibres by the massive  $\beta$ -phase

bridges were found in the AZ 91 - 20 vol.%Al<sub>2</sub>O<sub>3</sub>(f) composite [3]. A thicker zone in contact with the fibres was identified as fine magnesium (MgO) particles (Figure 5c), [3,5].

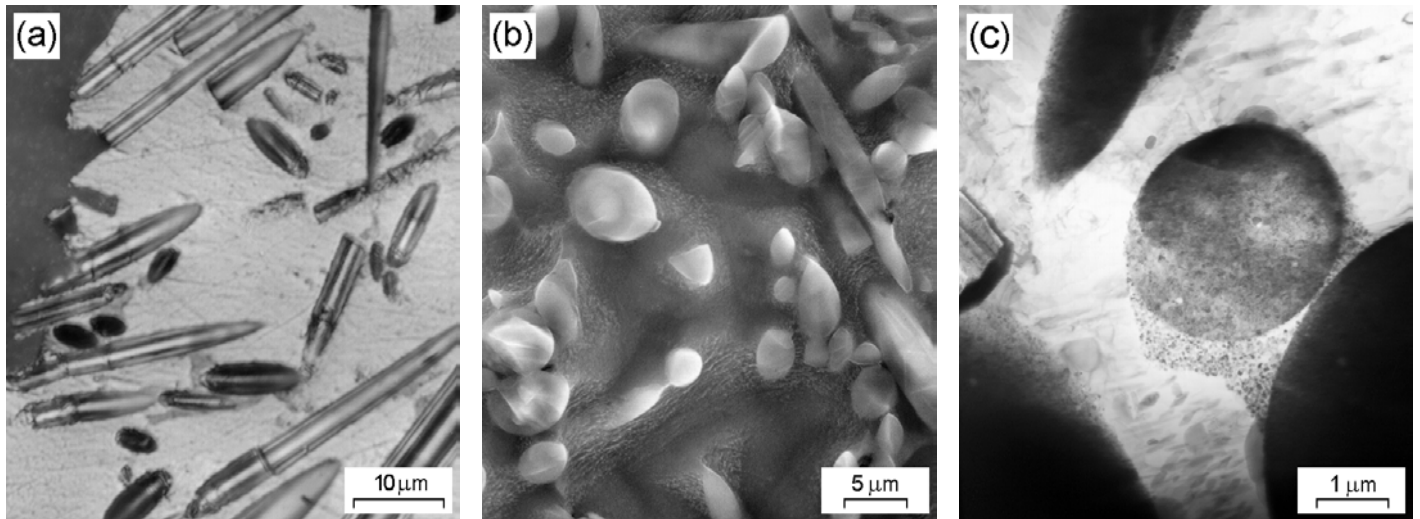


**Figure 5a,b,c:** Micrographs of the AZ 91-20 vol.%Al<sub>2</sub>O<sub>3</sub> (f) composite after creep: (a) fracture path (OM), (b) matrix-fibre interfaces (SEM, etched metallographic section), (c) matrix-fibre interfaces (TEM, foil).

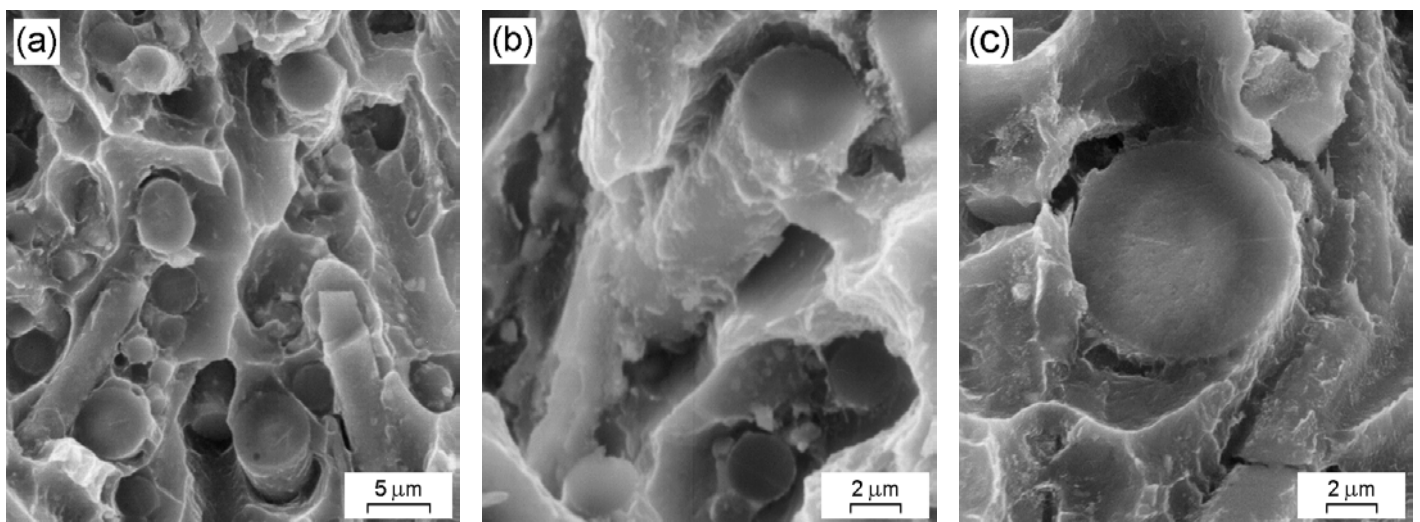


**Figure 6 a,b,c:** SEM micrographs of the QE 22-20vol.%Al<sub>2</sub>O<sub>3</sub> (f) composite showing creep fracture surface.

## DISCUSSION

It is relevant to discuss first the reason for different shapes of creep curves for the composite and the monolithic matrix alloy (Figs.1 and 2). The dominant primary stage apparent in the creep curves of the composite (Fig. 2) can be a result by non-linear visco-elastic deformation of the highly-stressed central regions of the fibres; this leads to a steady state due to matrix flow about the fibres when they are fully stretched elastically. Further, the occurrence of a lengthy primary stage of creep in the composite is probably associated with the additional secondary phase precipitation and with gradual change in the precipitate morphology during the creep exposure. Lastly, the observed long primary stages are not indicative of the initiation of any debonding at the interfaces between the matrix and the reinforcement and/or creep fibre breakage in accordance with the metallographic and fractographic observations. On the other hand, the tertiary creep behaviour should result from fibre fracture leading to a reduction in the fibre aspect ratio or the development of ductile tearing with off-loading of stress to the sound composite material, both factors leading to an acceleration in the creep rate. Thus, the observed extremely lengthy primary stage apparent in the creep curves of the composite in the present work does not support the prediction of the simplified

mechanistic model of creep in short fibre reinforced metal matrix composite [6] derived from the creep experiments and microstructural observations on short fibre reinforced aluminium alloys and based on three elementary microstructural processes including a multiple fibre breakage starting early in creep life. A possible explanation for this different creep behaviour in aluminium and magnesium short fibre reinforced metal matrix composites may lie in the different strength of the fibre-matrix interface (bonding) and load transfer during the creep of both composite materials.

As depicted in Fig. 3 the composites exhibit better creep resistance than the unreinforced matrix alloy; the presence of short-fibre reinforcement leads to reduced creep rate in the composite by two to three orders of magnitude. Such difference can arise when significant load transfer partitions the external load between the matrix and the reinforcement [3,4,7]. In the presence of load transfer the creep data may be successfully reconciled by putting the ratios of the creep rates of the composite and the matrix alloy equal to a factor given by  $(1-\alpha)^n$ , where  $\alpha$  is a load transfer coefficient having values lying within the range from 0 (no load transfer) to 1 (full-load transfer) [3,4]. The values of  $\alpha$  inferred from the data in Fig. 3 using  $n = 3$  [3] are within the range of 0.79 to 0.90. It is interesting to correlate these experimentally determined values  $\alpha$  with an analytical treatment. Kelly and Street [7] proposed a shear-lag approach that predicts the tensile creep behaviour of discontinuous fibre-reinforced composites. Subsequently, Nardone and Prewo [8] suggested a modified shear-lag model by considering the load transfer effect at the end of short fibres and various reinforcement geometries and arrangements (volume fraction, aspect ratio). The values of  $\alpha$  predicted from the modified shear-lag model with 20 vol. pct of short-fibre reinforcement are  $\alpha \cong 0.75$  and  $\alpha \cong 0.84$  for an experimentally observed fibre aspect ratios  $S$  (diameter/length)  $\sim 30$  and  $50$ , respectively. Thus, the predicted values are in reasonable agreement with the experimental values of  $\alpha$ .

## CONCLUSIONS

The creep resistance of squeeze cast AZ 91 and QE 22 magnesium alloys reinforced with 20 vol.%  $\text{Al}_2\text{O}_3$  short fibres is shown to be considerably improved compared to unreinforced matrix alloys. The direct strengthening effect of short fibre reinforcement arises mainly from effective load transfer. Direct strengthening dominates the creep behaviour of the composites due to good fibre/matrix interfacial bonding together with no substantial breakage of fibres during creep loading.

## ACKNOWLEDGEMENTS

Financial support for this work was provided by the Academy of Sciences of the Czech Republic under the Project K 1010104, by the Grant Agency of the Academy of Sciences of the Czech Republic under Grant A 2041902 and by Grant Agency of the Czech Republic under Grant 106/99/0187.

## REFERENCES

1. Edgar, R.L.(2000). In: *Magnesium Alloys and Their Applications*, pp. 3-8, Kainer,K.U.(Ed.), Weinheim.
2. Mordike, B.L. and Lukac, P.(1997).In: *Proc.3<sup>rd</sup> Int. Magnesium Conference*, pp.419-429, Lorimer G.W.(Ed), IOM, London.
3. Sklenicka, V., Pahutova, M., Kucharova, K., Svoboda, M. and Langdon, T.G. (2000). *Key Eng. Materials*, 171-174, 593.
4. Li, Y. and Langdon, T.G.(1999). *Metall.Mater.Trans.* 30A, 2059.
5. Pahutova, M., Sklenicka, V., Kucharova, K., Svoboda, M. and Langdon, T.G. (2001). In: *Proc.9<sup>th</sup> Int. Conference on Creep and Fracture of Engineering Materials and Structures*, Parker J.D. (Ed), University of Wales, Swansea, in press.
6. Dlouhy, A., Eggeler, G. and Merk, N. (1995). *Acta Met. Mater.*, 43, 535.
7. Kelly, A. and Street, K.N.(1972). *Proc. R. Soc. London*, 328A, 267.
8. Nardone, V.C. and Prewo, K.M.(1986) *Scripta Metall.*, 20, 43.